Diameter dependence of the electronic structure of ZnO nanorods determined by x-ray absorption spectroscopy and scanning photoelectron microscopy

J. W. Chiou, K. P. Krishna Kumar, J. C. Jan, H. M. Tsai, C. W. Bao, W. F. Pong,[a] and F. Z. Chien
Department of Physics, Tamkang University, Tamsui, Taiwan 251, Republic of China

M.-H. Tsai
Department of Physics, National Sun Yat-Sen University, Kaohsiung, Taiwan 804, Republic of China

I.-H. Hong,[b] R. Klauser, and J. F. Lee
National Synchrotron Radiation Research Center, Hsinchu, Taiwan 300, Republic of China

J. J. Wu and S. C. Liu
Department of Chemical Engineering, National Cheng Kung University, Tainan, Taiwan 701, Republic of China

(Received 16 April 2004; accepted 5 August 2004)

O *K*-, Zn L_3, and *K*-edges x-ray absorption near-edge structure (XANES) spectra and scanning photoelectron microscopy (SPEM) spectra were obtained for ZnO nanorods with various diameters. The analysis of the XANES spectra revealed increased numbers of O $2p$ and Zn $4p$ unoccupied states with the downsizing of the nanorods, which reflects the enhancement of surface states when the diameter is decreased. Valence-band photoemission spectra show a significant narrowing of the valence band for the 45 nm diameter nanorod. The Zn $3d$ intensities in the Zn $3d$ SPEM spectra are drastically diminished for all nanorods as compared to the ZnO reference film, which can be interpreted as a reduction in density of itinerant final states or in transition probability. © *2004 American Institute of Physics*. [DOI: 10.1063/1.1802373]

Zinc oxide (ZnO) II–VI semiconductor is an important material for optoelectronic applications.[1] ZnO nanorods and nanowires are particularly interesting because they can be used to tune electronic and optoelectronic devices that involve UV lasing action.[2,3] Knowledge of the electronic structure of the nanorods is crucial to understand the basic physics for these applications. Recently, Guo *et al.*[4] and Chiou *et al.*[5] have studied polarization-dependent O *K*-edge x-ray absorption and angle-dependent x-ray absorption near-edge structure (XANES) for highly oriented ZnO microrods and nanorods, respectively. To complement these studies, the present XANES and scanning photoelectron microscopy (SPEM) measurements focus on the dependence of the electronic structure on the diameter.

O *K*-, Zn L_3-, and *K*-edges XANES spectra and SPEM spectra were obtained at the National Synchrotron Radiation Research Center (NSRRC), Hsinchu, Taiwan. The O *K*-, Zn L_3-, and *K*-edges were measured in fluorescence mode using a high-energy spherical grating monochromator and wiggler-C beamlines. SPEM images and spectra were acquired at the U5-undulator beamline. The SPEM-end station at NSRRC has been described elsewhere.[6] Well-aligned ZnO nanorods were synthesized without a catalyst by low temperature chemical vapor deposition process using Si(100) as substrate. The details of the preparation of the ZnO nanorods are reported elsewhere.[7] The size distribution of the nanorods was investigated using a scanning electron microscope (SEM) and a transmission electron microscope (TEM). Three samples have been determined to have diameters of 150 ± 40, 80 ± 20, and 45 ± 10 nm and lengths of $\sim$600, 540, and 260 nm, respectively. These well-aligned nanorods have a hexagonal (wurtzite) structure and are oriented along the *c* axis as shown by the representative SEM and TEM micrographs for the 45 ± 10 nm nanorod in (a) and (b) of Fig. 1, respectively. X-ray diffraction (XRD) measurements of the ZnO nanorods and of a reference ZnO thin-film sample are displayed in Fig. 1. The characteristic peak of hexagonal ZnO with a (002) preferential orientation shows that the nanorods grow along the *c* axis.[7,8] The slight shift in the diffraction peak to lower angles for nanorods with smaller diameters was interpreted as an increase in the lattice spacing with respect to the growth direction.[9]

Figure 2 presents the O *K*-edge spectra of the well-aligned ZnO nanorods and the reference film. Features A_1, B_1, C_1, D_1, and E_1 are attributed to electron excitations from O $1s$ to $2p_\sigma$ (along the bilayer) and O $2p_\pi$ (along the *c* axis) states.[4,5,10–12] The upper inset is an enlargement of the O *K*-edge near-edge features obtained after subtracting the background using a best fitted Gaussian curve indicated by the dotted lines. The increase of the intensities of these features with the decrease of the diameter of the ZnO nanorod shows that the number of O $2p$ unoccupied states increases with the decrease of the diameter. The 528–531 eV energy range is magnified and shown in the lower inset. This inset reveals a shift to higher energies of the O *K*-edge for nanorods, which can be interpreted as a widening of the energy gap.

Figure 3 presents Zn L_3-edge XANES spectra of ZnO nanorods and the reference film. Features A_2, B_2, and C_2 are associated with the transition of Zn $2p$ electron to Zn $4s$ and antibonding $3d$ states.[5,13,14] The upper inset displays a mag-

[a]Author to whom correspondence should be addressed; electronic mail: wfpong@mail.tku.edu.tw
[b]Permanent address: Department of Applied Physics, National Chiayi University, Chiayi 600, Taiwan.

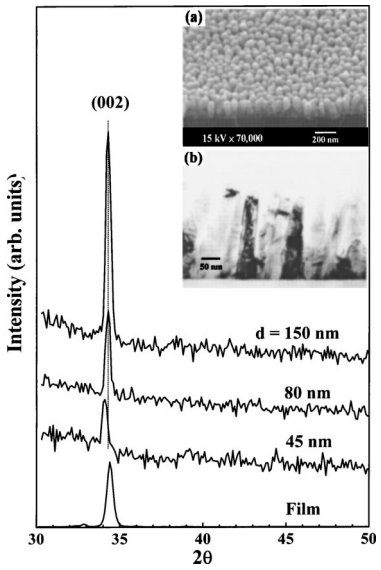

FIG. 1. XRD measurements of the well-aligned ZnO nanorods with 45, 80, and 150 nm diameters and the reference thin film, (a) and (b) show representative SEM and TEM images of the 45 nm nanorod, respectively

nified view of the near-edge features after background subtraction using a best fitted Gaussian curve indicated by the dotted lines. The upper inset reveals that the intensities of features B_2 and C_2 decrease with the decrease of the diameter, while the intensity of feature A_2 is less sensitive. Since $3d$ orbitals are more localized than the $4s$ orbital, the transition probability of Zn $2p \rightarrow 3d$ can be larger than that of Zn $2p \rightarrow 4s$. Then, features A_2, B_2, and C_2 will be dominated by Zn $3d$ state contributions. The decrease of the intensities shows a decrease of the number of Zn $3d$ antibonding states, which is consistent with a slight increase of the lattice spacing or Zn–O bond length observed in XRD measurements. The lower inset of Fig. 3 plots the integration of the intensities of the features in the O K- and Zn L_3-edges XANES spectra between 528 and 547 and 1012–1027 eV, respectively, which represent the numbers of O $2p$ and Zn $3d$ unoccupied states. The decrease of the number of Zn $3d$ unoccupied states with the decrease of the nanorod diameter

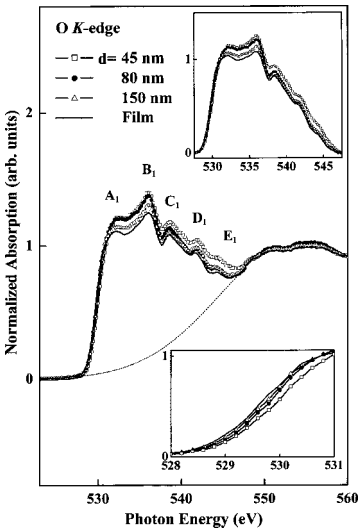

FIG. 2. O K-edge XANES spectra of the well-aligned ZnO nanorods with 45, 80, and 150 nm diameters and the reference thin film. The upper and lower insets show the magnified main features after background subtraction and the edge features, respectively.

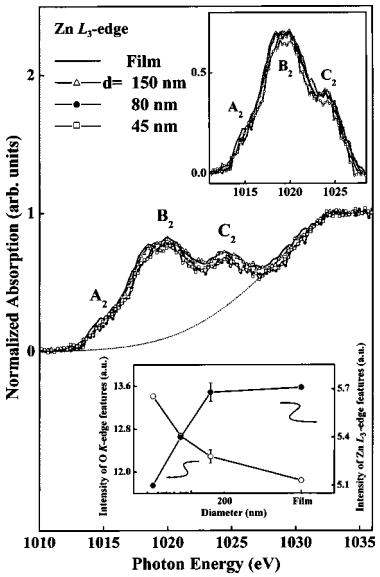

FIG. 3. (a) Zn L_3-edge XANES spectra of the ZnO nanorods with 45, 80, and 150 nm diameters and the reference thin film. The upper inset shows the magnified main near-edge features after background subtraction. The lower inset shows the integrated intensities of O K-(open circles) and Zn L_3-edges (filled circles) near-edge features.

suggests a reduction of the O $2p$–Zn $3d$ antibonding coupling with the downsizing of the nanorod.

Figure 4 presents the Zn K-edge spectra of the ZnO nanorods and the thin film. Features A_3, B_3, C_3, and D_3 reflect transition from Zn $1s$ to empty $4p_\pi$ (along c axis) and $4p_\sigma$ (along the bilayer) states.[8] These features are similar to those observed in the Ga K-edges XANES spectra of GaN thin film[15] and nanowires.[16] The magnified main peak B_3 shown in the inset exhibits an intensity increase as the nanorod diameter decreases. This result shows that the number of Zn $4p$ unoccupied states increases as the nanorod diameter decreases. One may interpret the decrease of the Zn $4p$ occupancy with the decrease of the nanorod diameter as a Zn $4p$–O $2p$ charge transfer. However, this interpretation will contradict with the increase of the number of O $2p$ un-

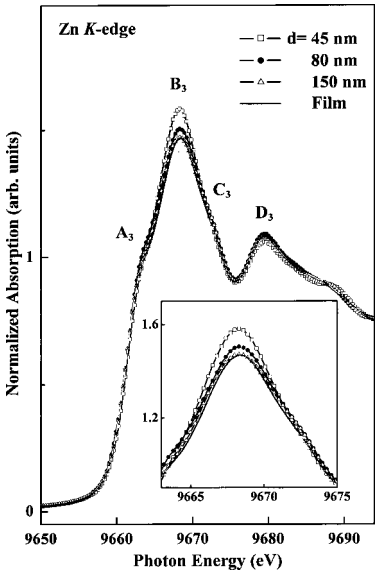

FIG. 4. Zn K-edge XANES spectra of the ZnO nanorods with 45, 80, and 150 nm diameters and the reference thin film. The inset shows the magnified feature B_3.

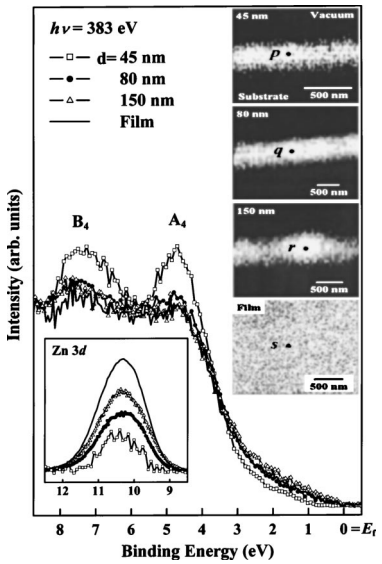

FIG. 5. Valence-band photoemission spectra obtained from selected positions *p*, *q*, *r*, and *s* shown in the upper inset, which shows the Zn 3*d* SPEM cross-sectional images of the well-aligned ZnO nanorods with 45, 80, and 150 nm diameters and the top view of the reference thin film, respectively. The lower inset presents the Zn 3*d* core-level spectra from positions *p*, *q*, *r*, and *s*.

occupied states shown in Fig. 2. A more reasonable interpretation is that the increase of both numbers of O 2*p* and Zn 4*p* unoccupied states shows an enhancement of near conduction-band-minimum surface states, because smaller diameter nanorods are expected to have a larger surface atom/interior atom number ratio.

Figure 5 displays spatially resolved valence-band photoemission spectra of the ZnO nanorods and the reference film. The Zn 3*d* SPEM images in this figure (insets) show the cross-sectional views of the nanorods and the top view of the reference film. The lower inset of Fig. 5 also exhibits the respective Zn 3*d* core-level spectra. The bright areas in the SPEM images correspond to the ZnO nanorods with a maximum Zn 3*d* intensity. The spectra displayed in Fig. 5 show photoelectron yields from selected positions indicated in the images as *p*, *q*, *r*, and *s*, which can be assigned to the sidewall regions of the ZnO nanorods with 45, 80, and 150 nm diameters and the top surface of the reference film, respectively. The zero energy refers to the Fermi level, E_f, which is the threshold of the emission spectrum. The spectra have two main features. Feature A_4 near the valence-band maximum is dominated by occupied O $2p-$Zn $4sp$ states and feature B_4 is associated with O 2*p* and Zn $3d/4sp$ hybridized states.[10,17–20] The figure demonstrates that the intensities of features A_4 and B_4 increase as the nanorod diameter decreases. The surface to volume ratio of a nanorod increases with the decrease of the diameter, so does the ratio of the number of surface atoms to the number of interior atoms. This increase may explain the larger SPEM intensity of the nanorods with smaller diameters. The intensity is substantially enhanced and the valence band is substantially narrowed for the 45 nm diameter nanorod.

The Zn 3*d* core-level photoemission spectra shown in the lower inset reveal a decrease in the peak intensity as the diameter of the nanorod decreases. Intuitively, this result can be interpreted as a decrease of the number of Zn 3*d* occupied states with the decrease of the diameter. However, this interpretation may not be correct because an isolated Zn atom has a filled 3*d* shell lying much lower than those of 4*s* and 4*p*. In ZnO, hybridization between O 2*p* and Zn 3*d* orbitals may give rise to unoccupied antibonding states. However, the intensity of the Zn 3*d* photoemission spectrum from the nanorod with the smallest diameter is less than half of that of the thin film. If the intensity directly reflects the Zn 3*d* occupancy, the Zn 3*d* photoemission results would imply that Zn 3*d* orbitals are less than half filled. This is very unlikely. The photoemission intensity is a product of the density of occupied Zn 3*d* states, density of unoccupied above vacuum-level itinerant states, and the transition probability between these states. Thus, the drastically reduced Zn 3*d* photoemission intensity for the nanorods is better interpreted as a drastically reduced density of the itinerant states and/or transition probability.

One of the authors (W.F.P.) would like to thank the National Science Council (NSC) of the Republic of China for financially supporting this research under Contract No. NSC 92-2112-M032-025.

[1]D. M. Bagnall, Y. F. Chen, Z. Zhu, T. Yao, S. Koyama, M. Y. Shen, and T. Goto, Appl. Phys. Lett. **70**, 2230 (1997); H. Cao, J. Y. Xu, D. Z. Zhang, S.-H. Chang, S. T. Ho, E. W. Seelig, X. Liu, and R. P. H. Chang, *ibid.* **84**, 5584 (2000).
[2]M. H. Huang, S. Mao, H. Feick, H. Yan, Y. Wu, H. Kind, E. Weber, R. Russo, and P. Yang, Science **292**, 1897 (2001).
[3]M. H. Huang, Y. Wu, H. Feick, N. Tran, E. Weber, and P. Yang, Adv. Mater. (Weinheim, Ger.) **13**, 113 (2001).
[4]J. H. Guo, L. Vayssieres, C. Persson, R. Ahuja, B. Johansson, and J. Nordgren, J. Phys.: Condens. Matter **14**, 6969 (2002).
[5]J. W. Chiou, J. C. Jan, H. M. Tsai, C. W. Bao, W. F. Pong, M.-H. Tsai, I.-H. Hong, R. Klauser, J. F. Lee, J. J. Wu, and S. C. Liu, Appl. Phys. Lett. **84**, 3462 (2004).
[6]R. Klauser, I.-H. Hong, T.-H. Lee, G.-C. Yin, D.-H. Wei, K.-L. Tsang, T. J. Chuang, S.-C. Wang, S. Gwo, M. Zharnikov, and J.-D. Liao, Surf. Rev. Lett. **9**, 213 (2002).
[7]J. J. Wu and S. C. Liu, Adv. Mater. (Weinheim, Ger.) **14**, 215 (2002); J. J. Wu and S. C. Liu, J. Phys. Chem. B **106**, 9546 (2002).
[8]E. Y. M. Lee, N. Tran, J. Russell, and R. N. Lamp, J. Appl. Phys. **92**, 2996 (2002).
[9]X.-D. Zhou and W. Huebner, Appl. Phys. Lett. **79**, 3512 (2001).
[10]E. P. Mikheeva, S. V. Koscheev, S. Ph. Ruzankin, G. M. Zhidomirov, S. A. Leontiev, V. G. Devjatov, and A. E. Cherkashin, J. Electron Spectrosc. Relat. Phenom. **94**, 59 (1998).
[11]P. J. Møller, S. A. Komolov, and E. F. Lazneva, J. Phys.: Condens. Matter **11**, 9581 (1999).
[12]J. G. Chen, B. Fruhberger, and M. L. Colaianni, J. Vac. Sci. Technol. A **14**, 1668 (1996).
[13]T. Mizoguchi, M. Yoshiya, J. Li, F. Oba, I. Tanaka, and H. Adachi, Ultramicroscopy **86**, 363 (2001).
[14]P. Schröer, P. Krüger, and J. Pollmann, Phys. Rev. B **47**, 6971 (1993).
[15]J. W. Chiou, S. Mookerjee, K. V. R. Rao, J. C. Jan, H. M. Tsai, K. Asokan, W. F. Pong, F. Z. Chien, M.-H. Tsai, Y. K. Chang, Y. Y. Chen, J. F. Lee, C. C. Lee, and G. C. Chi, Appl. Phys. Lett. **81**, 3389 (2002).
[16]J. W. Chiou, J. C. Jan, H. M. Tsai, W. F. Pong, M.-H. Tsai, I.-H. Hong, R. Klauser, J. F. Lee, C. W. Hsu, H. M. Lin, C. C. Chen, C. H. Shen, L. C. Chen, and K. H. Chen, Appl. Phys. Lett. **82**, 3949 (2003).
[17]L. Ley, R. A. Pollak, F. R. McFeely, S. P. Kowalczyk, and D. A. Shirley, Phys. Rev. B **9**, 600 (1974).
[18]W. Göpel, J. Pollmann, I. Ivanov, and B. Reihl, Phys. Rev. B **26**, 3144 (1982).
[19]R. T. Girard, O. Tjernberg, G. Chiaia, S. Söderholm, U. O. Karlsson, C. Wigren, H. Nylén, and I. Lindau, Surf. Sci. **373**, 409 (1997).
[20]K. Ozawa, K. Sawada, Y. Shirotori, K. Edamoto, and M. Nakatake, Phys. Rev. B **68**, 125417 (2003).